IEEE Photonics Journal
An IEEE Photonics Society Publication

Open Access

Properties of Garnet Monolayer Graphene Depolarizer

Volume 9, Number 3, June 2017

Xinbing Jiao
Yangfan Shen
Xinwei Zhao
Jing Wen

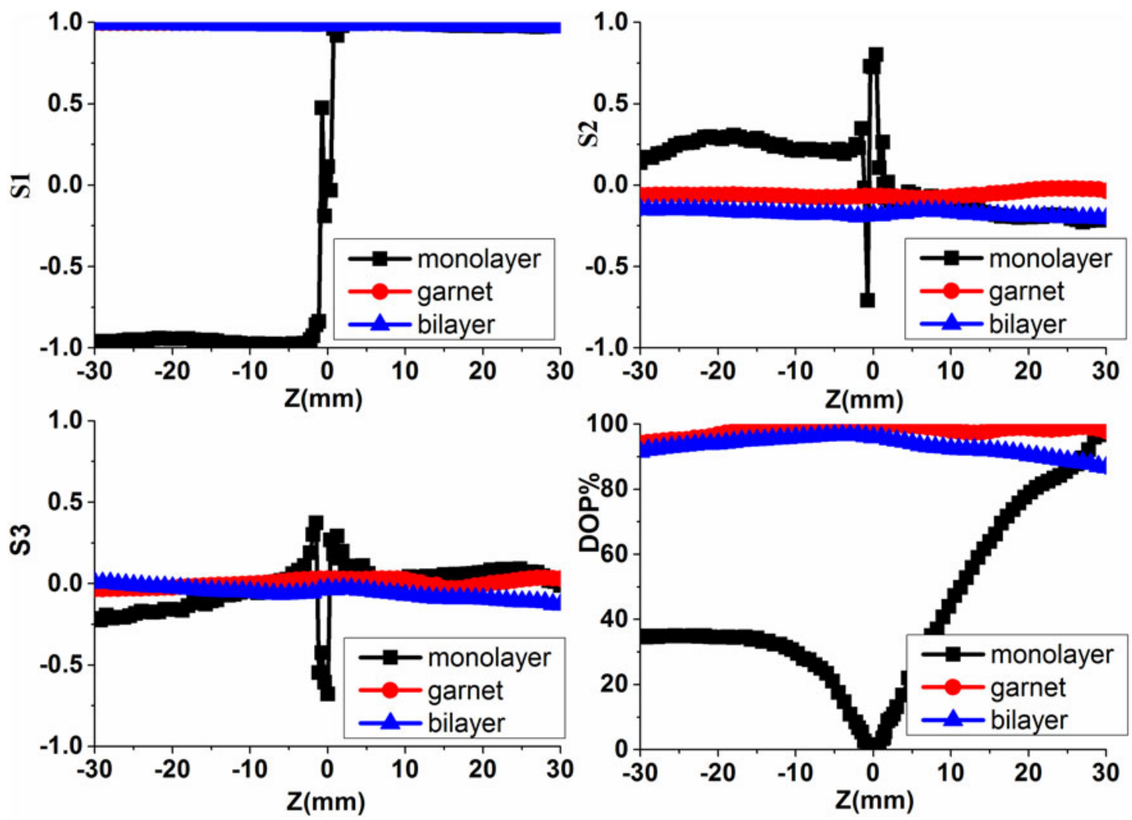

DOI: 10.1109/JPHOT.2017.2692216
1943-0655

Properties of Garnet Monolayer Graphene Depolarizer

Xinbing Jiao, Yangfan Shen, Xinwei Zhao, and Jing Wen

Shanghai Key Laboratory of Modern Optical System and Engineering Research Center of Optical Instrument and System, , Ministry of EducationUniversity of Shanghai for Science and Technology, Shanghai 200093, China

DOI:10.1109/JPHOT.2017.2692216

Manuscript received March 1, 2017; revised April 4, 2017; accepted April 5, 2017. Date of publication April 7, 2017; date of current version May 5, 2017. This work was supported in part by the Project of National Natural Science Foundation of China under Grant 61205076 and Grant 61378035; in part by the University Young Teacher Training Scheme of Shanghai, Hujiang Foundation of China, under Grant C14002; in part by the National Basic Research Program of China (973 Program) under Grant 2015CB352001; in part by the special-funded program on National Key Scientific Instruments and Equipment Development under Grant 2012YQ17000408; and in part by the 151 Talent Project of Zhejiang Province under Grant 12-2-008. Corresponding author: Xinbing Jiao (e-mail: xbjiao2011@gmail.com).

Abstract: A garnet monolayer graphene depolarizer is prepared by chemical vapor deposition (CVD). The characterizations of graphene on garnet are distinguished by Raman spectroscopy and Atomic Force Microscope (AFM). The z-scanning polarization properties of an input linearly polarized beam are measured by Stokes polarimeter, which passes through the garnet monolayer graphene depolarizer. The results show that the garnet monolayer graphene depolarizes the polarized beam into similar natural light and the degree of polarization of the input linearly polarized beam can be reduced from 100% to 0.1%, while the garnet and garnet with bilayer graphene cannot depolarize the polarized light. This work presents an interesting result on depolarization effect based on graphene when a laser beam passes through in perpendicular direction of graphene.

Index Terms: Optical and other properties, light-material interactions, sensors.

1. Introduction

The optical devices of depolarizer can reduce the degree of polarization (DOP) of a laser beam, independent of the polarization state of the input light [1]–[5]. A linearly polarized light can be transformed into similar natural light with the help of depolarizer, and this property is very important for designing optical devices. The DOP of the laser beam can be converted from a uniform polarization state to a varying polarization state by spatial polarization state scrambler or pseudo depolarizer which consist of two birefringent wedges, whose crystal axes were crossed at 90° [6]. Ning *et al.* reported that a rough-surfaced retardation plate based on matrix theory can modulate the polarization properties of a laser beam, which propagated in free space [7]. Ragheb *et al.* proposed two InGaAsP/InP compact integrated optical depolarizer, and DOP of the output light sources was less than 0.1 [8]. Yoon *et al.* measured the polarization changing speed of a beam by a simple depolarizer [9]. Zhang *et al.* reported that a wedge-shaped cell filled with cholesteric liquid crystal material can be used as depolarizer, the depolarizer was easily built and insensitive [10].

Garnet films can be widely used in data storage [11], Faraday isolator [12], polarization property micro-modulator [13], and direct current or alternating current sensors [14] due to their excellent physical and structural properties. Z-scanning method was popular used to study nonlinear properties of different materials for its simplicity, high sensitivity, and high precision [15], [16]. Wang theoretically analyzed and numerically demonstrated the influences of incident and polarization angles in the z-scan measurement [17]. The linearly polarized light was always used as the incidence beam in the Z-scanning system. There were less theoretical and experimental work investigated polarization effect of laser beams which went through depolarizer.

Some researchers have paid much attention on graphene as its exceptional optical and structural properties [18]. Bao *et al.* demonstrated a broadband fibre polarizer based on graphene, and showed strong s-polarization effects when a laser beam went through in parallel direction of graphene, due to the linear dispersion of Dirac electrons [19]. Zanini *et al.* discovered that the polarized properties of a polarized beam which went through in parallel or perpendicular direction of graphene were different [20].

In this paper, a garnet graphene depolarizer are prepared by chemical vapor deposition (CVD) method, and characterized by Raman spectroscopy, Atomic Force Microscope (AFM), and Stokes polarimeters. The optical polarization properties of the linearly polarized light which passes through a garnet graphene depolarizer, in perpendicular direction, are investigated by Z-scanning method. Further, the optical polarization properties of the linearly polarized light which passes through a quarter wave plate are also studied to determine whether the output light is similar natural light, when the garnet and garnet monolayer graphene moves in the $+$ z direction by the Z-scanning method.

2. Experimental Details

2.1 Preparation of Garnet Graphene

The garnet film (Granopt Co., Ltd) with a size of 0.39 mm $\times$ 3 mm $\times$ 3 mm is used as substrate. A garnet monolayer graphene and garnet bilayer graphene are prepared by CVD method. The growth processes of monolayer graphene are the following: first, loads the fused silica tube with a garnet, evacuates, back fill with H_2, heats to 1000 °C, and maintains a H_2 pressure of 5.33 Pa under the condition of 2 sccm flow for 60 min; second, heats the garnet substrate up to 1000 °C, and introduces 35 sccm of CH_4 for 100 min at a total pressure of 66.67 Pa; then, after exposure to CH_4, the furnace is cooled to room temperature. The bilayer graphene are prepared on garnet when the above processes are duplicated.

2.2 AFM and Raman Measurement

The monolayer and bilayer graphene grown on garnet are characterized by Nanoscope III Multimode AFM. Horiba JY Labram HR800 Raman spectrometer is used to identify the defects (D band), in-plane vibration of sp2 carbon atoms (G band) and the stacking orders (2-D band) [21], [22].

2.3 Optical Polarization Measurement

The optical polarization properties of the linearly polarized laser beam which passes through garnet, garnet monolayer graphene or garnet bilayer graphene as a function of the sample position in the z direction are measured by the experimental setup system of Fig. 1(a). As the thickness of the sample (garnet, garnet monolayer graphene, garnet bilayer graphene) is much smaller than the diffraction length of the linearly polarized focused laser beam. Research has shown that a lens can change the polarization properties of focused laser beam [23]. Therefore, the polarization properties of laser beam can be regarded as a function of focal length. In order to research the depolarization effect, the optical polarization properties of the linearly polarized laser beam which passes through the garnet, the garnet monolayer graphene or garnet bilayer graphenes, a quarter wave plate, in the $+$z direction are measured to determine whether the output light is similar natural light by the experimental setup system of Fig. 1(b). A linearly polarized laser is used as an optical source with a wavelength of 1550 nm. The laser beam passes through the lens, the sample (the

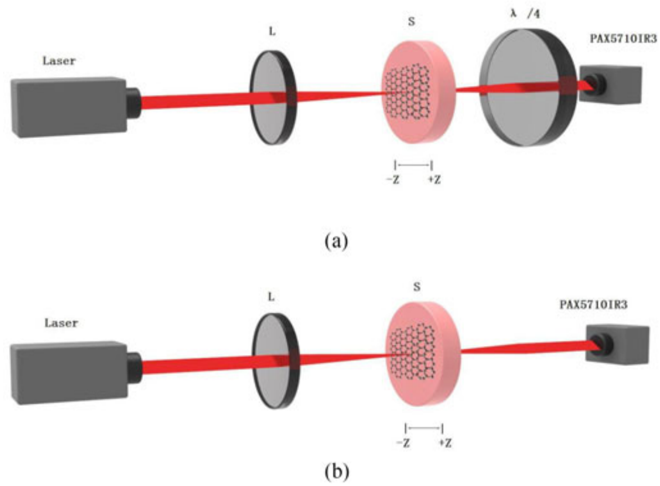

Fig. 1. Schematic diagram of experimental setup system. L, Lens; S, sample (garnet, garnet monolayer graphene, garnet bilayer graphenes); λ/4, 1/4 wave plate; PAX5710IR3, polarimeter.

garnet or the garnet monolayer graphene or the garnet bilayer graphenes), and the quarter wave plate, detected by PAX5710IR3 Stokes polarimeters. The samples'position can be moved from −30 mm to +30 mm in the z direction, and the precision of the z-scanning setup is 0.01 mm.

3. Theory

The polarization properties of polarized beam can be characterized by Stokes parameters and nonstationary parameters [24], [25]

$$S_{t0}(r,t) = J_{xx}(r,t) + J_{xx}(r,t) = I_x(r,t) + I_y(r,t) \tag{1}$$

$$S_{t1}(r,t) = J_{xx}(r,t) - J_{xx}(r,t) = I_x(r,t) - I_y(r,t) \tag{2}$$

$$S_{t2}(r,t) = J_{xy}(r,t) + J_{yx}(r,t) = I_\alpha(r,t) - I_\beta(r,t) \tag{3}$$

$$S_{t3}(r,t) = i[J_{yx}(r,t) - J_{yx}(r,t)] = I_r(r,t) - I_l(r,t). \tag{4}$$

The subscripts α, β relate to a coordinate system which rotates 45°. The subscripts r, l relate to right-circularly polarized and left-circularly polarized states. The Stokes parameter of polarized light, $S_{t0}(r,t)$ is the total intensity of light; $S_{t1}(r,t)$ is the intensity difference between horizontally polarized and vertically polarized light parts; $S_{t2}(r,t)$ is the intensity difference between +45°and −45° polarized parts; and $S_{t3}(r,t)$ is the intensity difference between right-circularly and left-circularly polarized parts.

The DOP of a polarized laser beam can be got from the following equation:

$$\mathrm{DOP}(r,t) = \frac{\mathrm{tr}J^{(pol)}(r,t)}{\mathrm{tr}J(r,t)} = \sqrt{1 - 4\frac{\det J(r,t)}{\mathrm{tr}^2 J(r,t)}} = \sqrt{2\frac{\mathrm{tr}J^2(r,t)}{\mathrm{tr}^2 J(r,t)} - 1}. \tag{5}$$

The DOP of a polarized laser beam can be different as function of time and space. The Stokes parameters $S_{ti}(r,t)$, i = 1,2,3 can be obtained from the following equation:

$$S_{ti}(r,t) = S_{ti}(r,t)/S_{t0}(r,t). \tag{6}$$

The DOP of a linearly polarized light can be represented geometrically by

$$\mathrm{DOP}_t^2(r,t) = \sum_{i=1}^{3} S_{ti}^2(r,t). \tag{7}$$

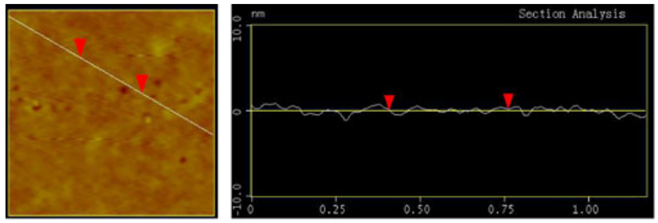

(a)

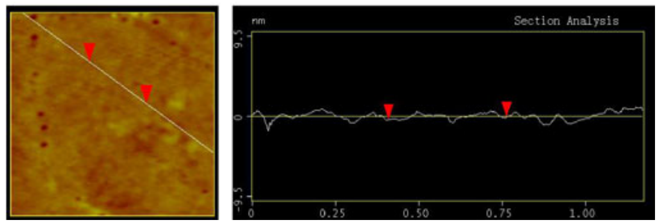

(b)

Fig. 2. AFM of monolayer (a) and bilayer grapheme (b).

The DOP of linearly polarized light is determined by the position in space when the instant of time is fixed. The polarization parameters, such as Stokes parameters S_1, S_2, S_3 and DOP of a laser beam, are more sensitive to anisotropic structure variations of graphene layer overlapping, boundary defects, sheet wrinkles and structural differences between graphene and substrates [26]. The precipitation process of CVD synthesis is nonequilibrium, it is extremely difficult to control the layer number of graphene on garnet [27]. The bilayer graphene grown on garnet are disorganized. The value of depolarization can be affected by scattering, and therefore, the structure change of graphene can vary the optical polarization properties of the linearly polarized light which passes through a graphene, while the optical polarization properties of the linearly polarized light which passes through double layer graphene are basely unchanged as the double layer graphene are disorganized.

4. Results and Discussion

4.1 AFM of Monolayer and Bilayer Graphene

The micro-structure and grain sizes of the monolayer and bilayer graphene on garnet, observed by AFM, were shown in Fig. 2(a) and (b). Fig. 2(a) shows the more detailed surface morphology with a 1 μm $\times$ 1 μm view of the monolayer graphene. The Root mean square (RMS) of monolayer graphene is 0.252 nm. The monolayer graphene is very flat. There are sparing particles on monolayer graphene. Fig. 2(b) shows the surface morphology with a 1 μm $\times$ 1 μm view of the bilayer graphene. There are spots and pores on bilayer graphene. The RMS of bilayer graphene is 0.313 nm. From Fig. 2(a) and (b), it can be seen that the surface of garnet monolayer graphene is much flatter than that of garnet bilayer graphene, and therefore, the scattering effect of garnet monolayer graphene is very weak.

4.2 Raman of Monolayer and Bilayer Graphene

The two Raman spectra are recorded in the same experimental conditions. Fig. 3 shows Raman spectra of garnet monolayer and garnet bilayer graphene. The major Raman features of garnet monolayer and garnet bilayer graphene are the so called G band (1582 cm^{-1}, 1585 cm^{-1}), and 2-D band (2684 cm^{-1}, 2691 cm^{-1}), respectively. The G band originates from in-plane vibration of

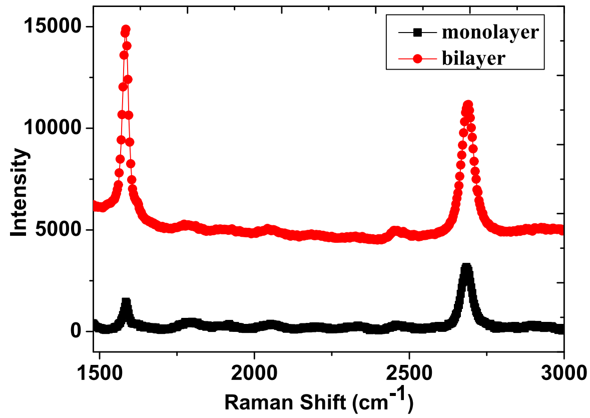

Fig. 3. Raman spectroscopy spectra of garnet monolayer and garent bilayer graphene.

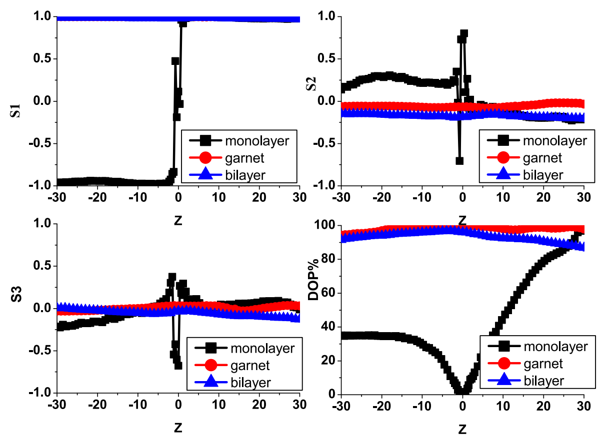

Fig. 4. Optical polarization properties of the polarized light which passes through the garnet (red), garnet monolayer graphene (black), and garnet bilayer graphene (blue).

sp2 carbons atoms [28], and the 2-D band derives from a two phonon double resonance Raman process [29] and indicates successful transfer to the garnet substrate.

4.3 Polarization Properties of Monolayer and Bilayer Graphene

The optical polarization properties of the linearly polarized light which passes through the garnet are obtained by PAX5710IR3 Stokes polarimeters, based on the man-made experimental setup system of Fig. 1(a), are shown in Fig. 4 (red), when the garnet moves in the z direction. The Stokes parameters of S_1 is about 1.0, while the Stokes parameters of S_2 and S_3 are about 0, respectively, shown in Fig. 4. The DOP of the output polarized light is about 100%, and is basically unchanged when the garnet moves in the Z-scanning process. Therefore, the input and the output light are linearly polarized when the light passes through the garnet. The garnet film can not be used as depolarizer.

The optical polarization properties of the linearly polarized light which passes through the garnet monolayer graphene are measured by the Stokes polarimeters PAX5710IR3 based on the man-made experimental setup system of Fig. 1(a) are shown in Fig. 4 (black), when the sample moves in the Z-scanning process. S_1 of Stokes parameters increases from $S_1 = -1.0$ (the garnet monolayer graphene moves from -30 mm to 0 mm in the Z-scanning process) to $S_1 = 1.0$ (the garnet monolayer graphene moves from 0 mm to 30 mm along the z direction). S_2 of Stokes parameters

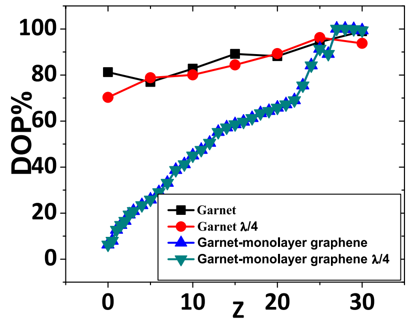

Fig. 5. The optical polarization properties of linearly polarized light which passes through the garnet, the garnet monolayer graphene and the quarter wave plate.

increases from $S_2 = 0.2$ (the garnet monolayer graphene moves from -30 mm to 0 mm in the Z-scanning process) to $S_2 = -0.2$ (the garnet monolayer graphene moves from 0 mm to 30 mm in the Z-scanning process). S_3 of Stokes parameters increases from $S_3 = -0.2$ (the garnet monolayer graphene moves from -30 mm to 0 mm in the Z-scanning process) to $S_3 = 0.2$ (the sample moves from 0 mm to 30 mm in the Z-scanning process). The Stokes parameters value of S_1, S_2, and S_3 have great changes when the garnet monolayer graphene in the $z = 0$ mm position, while the Stokes parameters have variations when the garnet monolayer graphene is near the $z = 0$ mm position. The DOP decreases from 40% (the garnet monolayer graphene moves from -30 mm to -15 mm) to 0.1% (the garnet monolayer graphene is in the $z = 0$ mm position), when the garnet monolayer graphene moves from -15 mm to 0 mm. Then, the DOP increases from 0.1% (the garnet monolayer graphene is in the $z = 0$mm position) to 100% (the garnet monolayer graphene is in the $z = 30$ mm position). The value of DOP is smaller, the depolarizer is better [8]. Obviously, the optical polarization property of a linearly polarized light can be depolarized due to the interaction between light and the monolayer graphene, as the graphene film is predominantly single-layer graphene and in regular arrangements [18]. The garnet with mono graphene can reduce the DOP of the linearly polarized light, and therefore, this sample can be used as a depolarizer.

Fig. 4 (blue) displays the relationship between the Stokes parameters and the position of the garnet bilayer graphene. The Stokes parameters of S_1, S_2, and S_3 are equal to 1.0, -0.14, and -0.03, respectively, and basically unchange when the garnet bilayer graphene moves from -30 mm to $+30$ mm in the Z-scanning process. The DOP equals to 95% and basically unchange when the sample moves in the Z-scanning process. Although, the graphene can be grown ideally from a single nucleation seed, the graphene grain boundaries are inevitably formed via stitching of graphene flakes and deteriorating the quality of graphene [30]. Therefore, the first layer graphene is neatly arranged, the second layer graphene is undisciplined with the first layer graphene, and the second layer graphene prepared on the garnet are not arranged in order. Therefore, the garnet with bilayer graphene can not modulate the DOP of polarized light.

As the depolarization effect of the garnet monolayer graphene only occurs in the $+z$ direction, the optical polarization properties of the linearly polarized light which passes through the sample (garnet or garnet monolayer graphene), a quarter wave plate (see Fig. 1(b)), are researched. From Fig. 5, it can be seen that the DOP of the linearly polarized light increases from 70% to 100%, when the linearly polarized light passes through the garnet and the quarter wave plate, and the sample moves in the $+Z$ direction. Therefore, the linearly polarized light which passes through the garnet and the quarter wave plate is also linearly polarized.

From Fig. 5, it displays that the DOP of the linearly polarized light increases from 6.3% to 100%, and the DOP of the linearly polarized light have the same trend, when the light passes through the garnet monolayer graphene, a quarter wave plate, and samples move from 0 mm to 30 mm. As we know, the linearly polarized light could be converted to the circularly polarized light when the linearly polarized light passes through a quarter wave plate, while the DOP of a natural light could not change. Therefore, the linearly polarized light which passes through the garnet monolayer graphene and the quarter wave plate is converted to similar natural light when garnet monolayer graphene moves in the $+z$ direction.

When comparing the DOP of the output polarized light from Figs. 4 and 5, it can be seen that the garnet monolayer graphene could affect the DOP of the input linearly polarized light, and the linearly polarized light can be converted into similar natural light. However, the DOP of the polarized light can not be converted when the light passes through the garnet and the garnet bilayer graphenes.

5. Conclusion

In conclusion, monolayer and bilayer graphene are prepared on garnet by CVD method. The properties of graphene films are characterized by the Raman spectroscopy and AFM. The optical polarization properties of the linearly polarized light which passes through the garnet, the garnet monolayer or the garnet bilayer graphenes, a quarter wave plate, in the perpendicular direction, are also investigated. The results indicate that the garnet monolayer graphene can depolarize the DOP of the linearly polarized laser beam from 100% to 0.1%, when the position of the garnet monolayer graphene moves in the Z-scanning process, while the garnet and the garnet bilayer graphenes can not. This is very important for designing optical devices.

References

[1] J. C. G. Sande, M. Santarsiero, G. Piquero, and F. Gori, "Longitudinal polarization periodicity of unpolarized light passing through a double wedge depolarize," *Opt. Exp.*, vol. 20, pp. 27348–27360, 2012.
[2] G. Biener, A. Niv, V. Kleiner, and E. Hasman, "Computer-generated infrared depolarizer using space-variant subwavelength dielectric grating," *Opt. Lett.*, vol. 28, pp. 1400–1402, 2003.
[3] C. Vena, C. Versace, G. Strangi, and R. Bartolino, "Light depolarization by non-uniform polarization distribution over a beam cross section," *J. Opt. A: Pure. Appl. Opt.*, vol. 11, 2009, Art. no. 125704.
[4] J. Carlos, G. De Sande, G. Piquero, and C. Teijeiro, "Polarization changes at lyot depolarizer output for different types of input beam," *J. Opt. Soc. Amer. A*, vol. 29, pp. 278–284, 2012.
[5] G. P. Agrawal and E. Wolf, "Propagation-induced polarization changes in partially coherent optical beams," *J. Opt. Soc. Amer. A*, vol. 17, pp. 2019–2023, 2000.
[6] S. C. Mcclain, R. A. Chipman, and L. W. Hillman, "Aberrations of a horizontal-vertical depolarizer," *Appl. Opt.*, vol. 31, pp. 2326–2331, 1992.
[7] N. Ma, S. G. Hanson, M. Takeda, and W. Wang, "Coherence and polarization of polarization speckle generated by a rough-surface retardation plate depolarizer," *J. Opt. Soc. Amer. A*, vol. 32, pp. 2346–2352, 2015.
[8] M. Ragheb, H. Elrefaei, D. Khalil, and O. A. Omar, "Design of an InGaAsP/InP compact integrated optical depolarizer," *Appl. Opt.*, vol. 54, pp. 9017–9024, 2015.
[9] I. Yoon, B. Lee, and S.-J. Park, "The polarization changing speed of the light depolarized by a simple depolarizer," *J. Light Technol.*, vol. 25, no. 7, pp. 1848–1853, Jul. 2007.
[10] D. Zhang *et al.*, "Cholesteric liquid crystal depolarizer," *Opt. Eng.*, vol. 46, 2007, Art. no. 70504.
[11] T. Nomura, M. Kishida, N. Hayashi, K. Iwasaki, and H. Umezawa, "An analytical model to study the transfer to magnetic pattern from videotape to garnet film," *IEEE Trans. Magn.*, vol. 48, no. 5, pp. 1863–1868, May 2012.
[12] K. Matsuda, H. Minemoto, K. Toda, O. Kamada, and S. Ishizuka, "Low-noise LD module with an optical isolator using a highly bi-substituted garnet film," *Electron. Lett.*, vol. 23, pp. 203–205, 1987.
[13] X. Jiao, J. Gao, and L. Chen, "Polarization modulation based on rotation of a garnet with grooved films," *Phys. Status Solidi A*, vol. 212, pp. 686–690, 2014.
[14] X. Jiao, T. G. Nguyen, B. Qian, C. Jiang, and L. Ma, "Faraday effect sensor redressed by $Nd_2Fe_{14}B$ biasing magnetic field," *Opt. Exp.*, vol. 20, pp. 1754–1759, 2012.
[15] X.-Q. Yan, Z.-B. Liu, X.-L. Zhang, W.-Y. Zhou, and J.-G. Tian, "Polarization dependence of Z-scan measurement: Theory and experiment," *Opt. Exp.*, vol. 17, pp. 6397–6406, 2009.
[16] H. Yan and J. Wei, "False nonlinear effect in Z-scan measurement based on semiconductor laser devices: Theory and experiments," *Photon. Res.*, vol. 2, pp. 51–58, 2014.
[17] X. Li *et al.*, "Large-area synthesis of high quality and uniform graphene films on Copper foils," *Science*, vol. 324, pp. 1312–1314, 2009.
[18] Q. Bao *et al.*, "Broadband graphene polarizer," *Nature Photon.*, vol. 5, pp. 411–415, 2011.
[19] M. Zanini, D. Grubisic, and J. E. Fischer, "Optical anisotropy of highly oriented pyrolytic graphite," *Phys. Status Solidi B Basic Res.*, vol. 90, pp. 151–156, 1978.
[20] S. Reich and C. Thomsen, "Raman spectroscopy of graphite," *Philos. Trans. Roy. Soc. A*, vol. 362, pp. 2271–2288, 2004.
[21] A. C. Ferrari *et al.*, "Raman spectrum of graphene and graphene layers," *Phys. Rev. Lett.*, vol. 97, 2006, Art. no. 187401.
[22] N. van Hulst, "Orienting out of a tight spot," *Nature Photon.*, vol. 1, pp. 208–209, 2007.

[23] M. Verma, P. Senthikumaran, J. Joseph, and H. C. Kandpal, "Experimental study on modulation of stokes parameters on propagation of a Gaussian schell model beam in free space," *Opt. Exp.*, vol. 21, pp. 15432–15437, 2013.

[24] P.-C. Chen, Y.-L. Lo, T.-C. Yu, J.-F. Lin, and T.-T. Yang, "Measurement of linear birefringence and diattenuation properties of optical samples using polarimeter and Stokes parameters," *Opt. Exp.*, vol. 17, pp. 15860–15884, 2009.

[25] X. Liu *et al.*, "Characterization of graphene layers using superresolution polarization parameter indirect microscopic imaging," *Opt. Exp.*, vol. 22, pp. 20446–20456, 2014.

[26] G. Wang *et al.*, "Synthesis of layer-tunable graphene: A combined kinetic implantation and thermal ejection approach," *Adv. Funct. Mater.*, vol. 25, pp. 3666–3675, 2015.

[27] Y. J. Lim *et al.*, "Monitoring defects on monolayer graphene using nematic liquid crystals," *Opt. Exp.*, vol. 23, pp. 14162–14167, 2015.

[28] M. A. Pimenta, G. Dresselhaus, M. S. Dresselhaus, and C. L. G. Jorio, "A study disorder in graphite based systems by Raman spectroscopy," *Phys. Chem. Chem. Phys.*, vol. 9, pp. 1276–1291, 2007.

[29] C. Thomsen and S. Reich, "Double resonant Raman scattering in graphite," *Phys. Rev. Lett.*, vol. 85, pp. 5214–5217, 2000.